The ISME Journal (2018) 12, 411–423

www.nature.com/ismej

ORIGINAL ARTICLE

Metabolic shift at the class level sheds light on adaptation of methanogens to oxidative environments

Zhe Lyu[1,2] and Yahai Lu[1,3]
[1]College of Resources and Environmental Sciences, China Agricultural University, Beijing, PR China; [2]Department of Microbiology, University of Georgia, Athens, GA, USA and [3]College of Urban and Environmental Sciences, Peking University, Beijing, PR China

Methanogens have long been considered strictly anaerobic and oxygen-sensitive microorganisms, but their ability to survive oxygen stress has also been documented. Indeed, methanogens have been found in oxidative environments, and antioxidant genes have been detected in their genomes. How methanogens adapt to oxidative environments, however, remain poorly understood. Here, we systematically predicted and annotated antioxidant features from representative genomes across six well-established methanogen orders. Based on functional gene content involved in production of reactive oxygen species, Hierarchical Clustering analyses grouped methanogens into two distinct clusters, corresponding to the Class I and II methanogens, respectively. Comparative genomics suggested a systematic shift in metabolisms across the two classes, resulting in an enrichment of antioxidant features in the Class II. Moreover, meta-analysis of 16 S rRNA gene sequences obtained from EnvDB indicated that members of Class II were more frequently recovered from microaerophilic and even oxic environments than the Class I members. Phylogenomic analysis suggested that the Class I and II methanogens might have evolved before and around the Great Oxygenation Event, respectively. The enrichment of antioxidant features in the Class II methanogens may have played a key role in the adaption of this group to oxidative environments today and historically.
The ISME Journal (2018) **12,** 411–423; doi:10.1038/ismej.2017.173; published online 14 November 2017

Introduction

Methane has been a key component in the atmosphere since the dawn of life on Earth (Kasting, 1993). Being one of the most potent greenhouse gases, methane has a crucial role in regulating the modern as well as ancient climate of Earth (Pavlov *et al*., 2000). Snowball events in the ancient Earth could be linked to declines in the concentration of methane, and modern Earth is now experiencing global warming at least in part owing to excess emissions of anthropogenic methane (Kasting, 2004; Bousquet *et al*., 2006). The biological production of methane in the atmosphere has been largely attributed to the activity of methanogens, a group of strictly anaerobic microbes which likely originated at some point in the mid to early-Archean (Battistuzzi *et al*., 2004; Ueno *et al*., 2006; Wordsworth and Pierrehumbert, 2013). It is suggested that methanogens could have dominated the biosphere in most of the Archean Eon, and methane emissions may have prevented the rapid cooling of the early Earth (Catling *et al*., 2001). However, populations of methanogens appeared to decline greatly at the end of the Archean Eon, likely due to the depletion of oceanic nickel, which is an essential cofactor for many key enzymes in the methanogenesis pathway and required for growth (Thauer *et al*., 2010), and the increasing environmental oxygenation during the Great Oxidation Event at ~2.5–2.3 Ga (Konhauser *et al*., 2009). Oxygenation could be detrimental directly to methanogens via the formation of deadly derivatives of O_2 or reactive oxygen species (ROS), such as H_2O_2 and O^{2-} radicals (Imlay, 2008).

Previous reports have demonstrated that methanogens neither abandon their overall dependence on nickel nor develop nickel-specific ligands to cope with low nickel availability when facing nickel famine (Hausrath *et al*., 2007; Thauer *et al*., 2010). Likewise, it remains elusive how ancestors of methanogens coped with the ROS damage. Nevertheless, they appeared to have survived those catastrophic events and proliferated into the modern era. Today, modern methanogens are virtually found in all types of anaerobic environments, and most of them are sensitive to oxygen (Fetzer *et al*., 1993; Fetzer and Conrad, 1993; Thauer *et al*., 2010; Yuan *et al*., 2011). However, it has been shown that some methanogens could survive

Correspondence: Y Lu, College of Urban and Environmental Sciences, Peking University, Beijing 100871, PR China.
E-mail: luyh@pku.edu.cn
Received 19 April 2017; revised 31 July 2017; accepted 9 August 2017; published online 14 November 2017

oxygen stress for several hours to days (Kiener and Leisinger, 1983; Fetzer *et al*., 1993; Ueki *et al*., 1997; Ma and Lu, 2011), and they have also been found in typical oxidative environments such as upland soils (Angel *et al*., 2011; Angel *et al*., 2012). Likewise, physiological, ecological and genomic analyses have revealed that at least certain methanogen lineages have evolved strong antioxidant features (Fetzer and Conrad, 1993; Erkel *et al*., 2006; Angel *et al*., 2012; Lyu and Lu, 2015). However, how methanogens adapt to oxidative environments remain poorly understood. To gain more insight into this puzzle, here we sampled genomes from six well-established methanogen orders (*Methanobacteriales*, *Methanocellales*, *Methanococcales*, *Methanomicrobiales*, *Methanosarcinales* and *Methanopyrales*) and predicted their antioxidant features by analyzing functional genes relevant to ROS production, O_2/ROS elimination and self-repairing systems. A survey of environmental 16 S rRNA genes of those methanogen lineages was also conducted to determine their distribution in oxidative environments. At last, a phylogenomic analysis was performed to estimate major diversification events of those methanogens and to put our results into an evolutionary perspective.

Subjects and Methods

Comparative genomics

Functional genes associated to antioxidant potentials were extracted from the sampled methanogen genomes (Supplementary Table 1) and manually curated and re-annotated based on experimental evidence (Supplementary Methods). The presence of [4Fe-4S] clusters in methanogenesis redox enzymes was summarized from various experimental sources and verified via examining conserved [4Fe-4S] binding motifs for all strains by sequence alignments (Major *et al*., 2004). Hierarchical clustering of gene content was done by the Ward's minimum variance method with JMP Pro, Version 12, SAS Institute Inc. Nonparametric tests were performed with Kruskal–Wallis analysis of variance followed by Mann–Whitney to investigate the statistical differences in gene abundance among methanogen classes.

Environmental gene survey

Environmental 16 S rRNA gene sequences were extracted from EnvDB and classified by RDP10 (Cole *et al*., 2009; Tamames *et al*., 2009). Habitat information was further extracted and verified from the literature as well as GenBank for each sequence. Complete methods and datasets were summarized in Supplementary Information.

Phylogenetic analysis

Genome sequences were sampled from IMG/ER (https://img.jgi.doe.gov/cgi-bin/mer/main.cgi). Genes encoding the 22 ribosomal proteins were extracted from the sampled genomes (Supplementary Table 1). Ribosomal proteins were aligned by MAFFT (v7.107) (Katoh and Standley, 2013). Concatenation of sequence data was done by Geneious R8.1 (Kearse *et al*., 2012). The E-INS-I algorithm was used for MAFFT. The alignments were filtered by eliminating any position that was missing data from 90% or more out of the total aligned taxa unless otherwise mentioned. Phylogenetic trees were constructed by either RAxML (v8.2.9) constrained by the bootstrapping autoMRE stopping criteria or MrBayes (v3.2.6) through Bayesian inference (BI) (Ronquist and Huelsenbeck, 2003; Stamatakis *et al*., 2008). Both algorithms were hosted by the CIPRES Science Gateway (Miller *et al*., 2010), where a WAG protein matrix model with corrections for a gamma distribution with four discrete rate categories and a proportion of invariant sites (WAG+G+I) were implemented for the phylogenetic analyses. Whenever necessary, another protein model (LG+G+I) was also implemented in both RAxML and MrBayes, testing if a tree topology remained robust after changing the substitution model. This model was chosen out of the 56 different substitution models examined by Mega 7 based on the best fit Bayesian Information Criterion (Kumar *et al*., 2016). For BI, the following parameters were also implemented, nrun = 3, ngen = 1 000 000, nchains = 4, samplefreq = 10, nst = 6, Nucmodel = protein, rates = invgamma, sump burnin = 50 000, sumt burnin = 50 000 and burin frac = 0.25. A few pre-runs were performed to optimize the parameters to ensure the log probability plateaued after the burnin setting and the Markov Chain Monte Carlo samplings converged before the ngen setting.

Both RAxML and MrBayes trees were subjected to molecular dating with the RelTime module in Mega 7 (Tamura *et al*., 2012; Kumar *et al*., 2016). Relative node ages were first obtained by using the ribosomal protein alignment data with the same aforementioned WAG+G+I or LG+G+I model in a maximum-likelihood framework. Reliable calibration anchors reported previously were then used to scale the relative node ages into absolute dates (Battistuzii and Hedges, 2009; Marin *et al*., 2017). RelTime belongs to the latest version of molecular dating algorithms, which appears to outperform the sophisticated and time-consuming Bayesian methods while retaining comparable accuracy (Tamura *et al*., 2012; Kumar and Hedges, 2016).

Results and discussion

Antioxidant features across methanogens

Three strategies could be envisaged to respond to the oxygenation challenge: (i) limiting ROS production, (ii) reducing accumulation of ROS within the cell and (iii) self-repairing for ROS damage. Studies have revealed that all strategies are essential to ensure survival of both aerobes and anaerobes under oxidative stress (Gort and Imlay, 1998; Imlay, 2002; Hillmann *et al*., 2008; Imlay, 2008). Accordingly, we

retrieved the functional genes involved in these strategies from methanogen genomes, and the results shown below grouped those methanogens into two clusters based on their distinct antioxidant features.

ROS production. The amount of ROS production is mainly related to the presence of quinone-derived electron carriers and [4Fe-4S] clusters in the central metabolism (Imlay, 2002). This is owing to the formation of superoxide (O_2^-) and hydrogen peroxide (H_2O_2) when oxygen reacts with the quinone-like electron carriers (for example, flavin and ubiquinone) (Müller, 1987; Massey, 1994). The reactivity of oxygen with those electron carriers is owing to the formation of semiquinone derived radicals (for example, flavosemiquinone and ubisemiquinone) (Müller, 1987; Massey, 1994). The H_2O_2 further oxidizes [4Fe-4S] clusters and generates hydroxyl radicals (HO·) by the Fenton reaction (Walling, 1975).

Being the hub of energy production and biosynthesis, the methanogenesis pathway is probably the main source for ROS production. Hierarchical Clustering analyses based on functional gene content revealed two different clusters (Figure 1). The two clusters correspond to the Class I and II methanogens proposed by the Brochier-Armanet group (Brochier-Armanet *et al*., 2011; Petitjean *et al*., 2015). The Class I methanogens include *Methanobacteriales*, *Methanococcales* and *Methanopyrales*, while the Class II comprises *Methanocellales*, *Methanomicrobiales* and *Methanosarcinales*. Therefore, a systematic shift in gene content patterns for methanogenesis would likely be associated with the evolution of methanogens at the class level.

This shift could potentially reduce the ROS production for the Class II methanogens through two different mechanisms in the methanogenesis pathway. One, the Class I methanogens use a flavin/ferrodoxin mediated electron bifurcation mechanism (Thauer *et al*., 2008; Kaster *et al*., 2011), whereas the Class II *Methanosarcinale*s mainly use a cytochrome/methanophenazine-mediated electron transfer mechanism for methanogenesis (Table 1 and Supplementary Table 2) (Welander and Metcalf, 2005; Thauer *et al*., 2008; Kulkarni *et al*., 2009). The electron bifurcation mechanism requires the formation of flavosemiquinone, which could react with oxygen to form O_2^- and H_2O_2 (Buckel and Thauer, 2012). In hydrogenotrophic *Methanosarcinales* spp., flavin proteins are not involved in the cytochrome/methanophenazine mechanism (Welander and Metcalf, 2005). In aceticlastic and methylotrophic *Methanosarcinales* spp., a Fpo or Rnf flavin protein complex participates in the electron transfer (Kulkarni *et al*., 2009; Spring *et al*., 2010; Schlegel *et al*., 2012). However, current evidence favors a direct electron transfer instead of an electron bifurcation mechanism for the Fpo or Rnf complex, which would not require a formation of flavosemiquinone (Catlett *et al*., 2015). A bifurcation mechanism has recently been proposed for the cytoplasmic Hdr complex, but it may only play an auxiliary role when needed for maximal thermodynamic efficiency (Yan *et al*., 2017). Two, although the Class II *Methanomicrobiales* and *Methanocellales* have been predicted to use the bifurcation mechanism, they reduce their [4Fe-4S] motifs by about 70% in their methanogenesis pathway compared to the Class I methanogens (Table 1). This could reduce HO· production through the Fenton reaction. This view was supported by the Hierarchical Clustering analysis that showed *Methanomicrobiales* and *Methanocellales* merged into the Class I once enzymes with reduced numbers of [4Fe-4S] motifs were removed from the bifurcation-based methanogenesis pathway (Supplementary Figure 1). Likewise, Hierarchical Clustering solely based on those [4Fe-4S] enzymes separated *Methanomicrobiales* and *Methanocellales* from the Class I (Supplementary Figure 2). Interestingly, the same analysis now moved *Methanosarcinales* into the Class I, suggesting an unexpected link between *Methanosarcinales* and the Class I methanogens in the context of [4Fe-4S] enzymes (Supplementary Figure 2).

O_2/ROS elimination. O_2/ROS elimination is achieved by a variety of antioxidant enzymes in model microbes (Imlay, 2008; Imlay, 2013). By working together, these enzymes can reduce O_2 to H_2O, and transform H_2O_2 and O_2^- into less-toxic products such as O_2 and H_2O. HO^- can only be indirectly eliminated by reducing HO^- production via iron storage to avoid the Fenton reaction (Neilands, 1993; Touati *et al*., 1995). Many of such eliminations are redox-dependent reactions and require reducing power to proceed, which usually comes directly from small redox proteins (Lu and Holmgren, 2014). These redox proteins also serve as a buffering system to keep cellular redox system from becoming overly oxidized (Susanti *et al*., 2014).

Overall, common O_2/ROS elimination enzymes were present in all methanogens regardless of class affiliation except for the complete absence of catalase in the Class I methanogens (Table 2 and Supplementary Table 3). However, Class II methanogens possessed statistically more genes encoding antioxidant enzymes and small redox proteins than their Class I counterparts. These observations suggest that a core pool of antioxidant genes is shared by both classes of methanogens, but this pool expands numerically in the Class II methanogens. However, the statistical difference for this expansion disappeared after correction for genome size. The genomes of the Class II methanogens were ~1.7 times larger than those of the Class I methanogens (Table 2). In other words, the genome size and the pool of antioxidant genes expand by the same extent in the Class II methanogens. On one hand, the expansion of antioxidant gene set could simply be a byproduct of genome expansion. If this is true, an

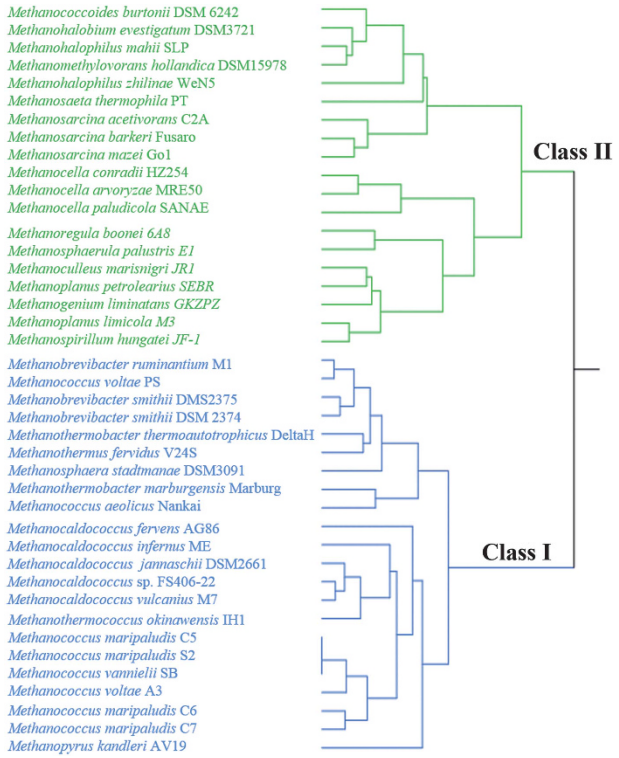

Figure 1 Hierarchical clustering topology for the methanogenesis gene content (Supplementary Table 2) among the methanogens, which are color coded as blue and green, corresponding to the previously proposed Class I and Class II methanogens (Brochier-Armanet *et al.*, 2011; Petitjean *et al.*, 2015), respectively. The clustering was done by the Ward's minimum variance method with JMP Pro.

across-the-board expansion of antioxidant genes would be expected. Apparently, this did not happen, and the $F_{420}H_2$ oxidase even exhibited a reduction (Table 2). On the other hand, a numerical expansion of certain but not all antioxidant genes in the Class II methanogens could reflect a specific adaptation to oxidative environments.

Four specific observations support this latter view (Table 2). (i) Both $F_{420}H_2$ oxidase and NO/O_2 reductase oxidize O_2 into H_2O, but the latter has a much higher K_m for O_2 (Gomes *et al.*, 2002; Silaghi-Dumitrescu *et al.*, 2005), whereas the former is deactivated when cells are exposed to air (Seedorf *et al.*, 2004, 2007). In addition, NO/O_2 reductase detoxifies NO, an inhibitor of methanogenesis which could be abundant at the oxic-anoxic interface (Klüber and Conrad, 1998; Rodrigues *et al.*, 2006). The almost absence of $F_{420}H_2$ oxidase in the Class II methanogens is striking given that these methanogens still use $F_{420}H_2$ as main electron carriers for methanogenesis (Welander and Metcalf, 2005). Therefore, a shift from $F_{420}H_2$ oxidase dominance in the Class I methanogens to NO/O_2 reductase dominance in the these methanogens could suggest an adaptation of the Class II members to oxidative conditions (Table 2 and Supplementary Figure 3). (ii) Rubredoxin and thioredoxin are small redox proteins that have been shown to have important roles in a variety of antioxidant processes for methanogens (Susanti *et al.*, 2014). Thioredoxin is a stronger reducing agent than rubredoxin, transferring electrons at redox potentials ~ -300 to -120 mV and 0 ± 100 mV, respectively (Åslund *et al.*, 1997; Balmer *et al.*, 2004; Lin *et al.*, 2005). Compared with the Class I methanogens, the rubredoxin system is numerically comparable while the thioredoxin system is substantially expanded in the Class II methanogens (Table 2), indicating a potential enhancement of the redox-buffering system in the Class II members. (iii) Transmembrane thioredoxin proteins were also commonly predicted in the Class II methanogens, but rarely in the Class I methanogens (Table 2). In addition to the thioredoxin domain present either in the cytoplasmic or periplasmic side, those transmembrane thioredoxin proteins also have two or three cysteine residues in the transmembrane region, located within the vicinities of both sides of the membrane (Figure 2). It has been previously shown that electron transfer could happen between those cysteine residues and the thioredoxin domain (Krupp *et al.*, 2001; Deshmukh *et al.*, 2003). Therefore, the transmembrane thioredoxin proteins may enable electron shuffle between the cytoplasmic and periplasmic spaces, which may help with redox recovery around the cellular membranes under oxidative stress (Figure 2). And (iv), the Class I methanogens appear to use $F_{420}H_2$ to regenerate the reduced thioredoxin, whereas the Class II methanogens probably use NADPH or NADH instead (McCarver and Lessner, 2014; Susanti *et al.*, 2016). Although $F_{420}H_2$ may be an efficient electron donor when H_2 levels were high in the atmosphere of an ancient and anoxic Earth, it would not be as good as NADPH or NADH in the face of an oxygenated Earth where H_2 levels were low (Nisbet and Sleep, 2001; Lollar *et al.*, 2014). Not only is it less likely to be reduced at lower H_2 concentrations, but it reacts chemically with O_2 and, thus is less stable than NADPH and NADH under oxidative conditions (Seedorf *et al.*, 2004; Susanti *et al.*, 2016).

Self-repairing system. ROS damages DNA bases by oxidizing purines and pyrimidines and is mutagenic (Dalhus *et al.*, 2009). It also oxidizes membrane lipids into phospholipid hydroperoxides and reacts with sulfur amino acids of proteins to form disulfide bonds or methionine sulfoxide, leading to dysfunction of membrane and protein structures (Manevich *et al.*, 2002; Weissbach *et al.*, 2005). In addition, ROS causes iron release from iron–sulfur (FeS) clusters (Djaman *et al.*, 2004). Cells can repair these damages to DNA, lipids, protein and FeS clusters via DNA base repair, phospholipid hydroperoxides reduction, disulfide bonds (S–S) and sulfoxide moiety (S = O) reduction, and FeS assembly, respectively.

Genes encoding DNA base repair, S–S and S = O reduction enzymes were either moderately or strongly enriched in the Class II methanogens

Table 1 Redox enzymes potentially contributing to ROS production from methanogenesis pathways

Class	*Pathway*	*Reactions (electron donor)*	*Enzymes*	*Total*[a] *[4Fe-4S]*
I	Hydrogenotrophic	Fd_{ox} reduction ($H_2 + \Delta\mu Na^+$)	Eha[b] & Ehb	34
		CO_2 reduction (Fd_{red})	Fmd	46[c]
		CoB-S-S-CoM reduction & energy conservation (H_2)	Mvh+HdrABC	21
II	Hydrogenotrophic	Fd_{ox} reduction ($H_2 + \Delta\mu Na^+$)	Eha[d]/Ech/Mbh[e]	3
		CO_2 reduction (Fd_{red})	Fmd	46[c]
		CoB-S-S-CoM reduction & energy conservation (H_2)	? + Hdr[f]	9
			Mvh + HdrABC	8
			Vht + HdrDE[g]	5
	Aceticlastic	Fd_{ox} reduction (Acetyl-CoA)	ACS/CODH	52[c]
		CoB-S-S-CoM reduction & energy conservation (H_2 or Fd_{red})	Vht + HdrDE	5
			Rnf + HdrDE	9
			Fpo(Fd) + HdrDE	6
	Methylotrophic	Fd_{ox} reduction (CHO-MFR)	Fmd	46[c]
		CoB-S-S-CoM reduction & energy conservation (H_2 or Fd_{red} or $F_{420}H_2$)	Vht + Hdr	6
			Vht & Fpo (F_{420}) + HdrDE	11
			Rnf & Fpo (F_{420}) + HdrDE	13

Abbreviations: ACS/CODH, carbon monoxide/acetyl CoA synthase; CoB-S-S-CoM, heterodisulfide co-enzyme B and co-enzyme M; CHO-MFR, formylmethanofuran; Eha, Ehb, Ech and Mbh, membrane bound energy converting hydrogenases homologous to each other; Fd_{ox} and Fd_{red}, oxidized and reduced ferredoxin, respectively; Fmd, formylmethanofuran dehydrogenase; Fpo, membrane bound $F_{420}H_2$ dehydrogenase; HdrABC and HdrDE, soluble and membrane bound heterodisulfide reductase, respectively; Mvh and Vht, soluble and membrane bound F_{420}-non-reducing hydrogenase, respectively; Rnf, membrane bound *Rhodobacter* nitrogen fixation complex. Note, Ech in acetotrophic and methylotrophic pathways was not listed here for the sake of simplicity. See Supplementary Table 2 for more details about gene re-annotation, enzymes comparison and [4Fe-4S] clusters data.

[a]If a protein structure is not available, the values assume each subunit in the protein present in the form of a monomer.

[b]Not present in *Methanosphaera stadtmanae*.

[c]Data obtained from protein structures.

[d]Present only in *Methanospirillum hungatei, Methanoculleus marisnigri, Methanoplanus petrolearius, Methanoplanus limicola* and *Methanofollis liminatans*.

[e]Present only in *M. hungatei, M. petrolearius, M. limicola* and *M. liminatans*.

[f]A bifurcation mechanism similar to the Mvh/Hdr complex has been hypothesized for *Methanomicrobiales*, but the identity of the hydrogenase remains elusive (Thauer *et al*., 2010).

[g]Present only in *Methanosarcina* spp.

Table 2 Comparison of gene abundance for O_2/ROS elimination enzymes between the Class I and Class II methanogens

Function	*Enzyme*	*Number of genes ± s.e.m.*	
		Class I	*Class II*
$2\ H_2O_2 \rightarrow O_2 + 2\ H_2O$	Catalase[a]	0	0.8 ± 0.2
$H_2O_2 + 2\ e + 2\ H^+ \rightarrow 2\ H_2O$	Peroxiredoxin[a,b]	0.7 ± 0.2	3.0 ± 0.7
	Rubrerythrin	2.0 ± 0.1	2.2 ± 0.3
$2\ O_2^- + 2\ H^+ \rightarrow\ H_2O_2 + O_2$	Superoxide dismutase[a]	0.1 ± 0.1	0.7 ± 0.2
$O_2^- + 2\ H^+ \rightarrow H_2O_2$	Superoxide reductase	1.0 ± 0.1	1.2 ± 0.2
$O_2 + 2\ F_{420}H_2 \rightarrow 2\ F_{420} + 2\ H_2O$	$F_{420}H_2$ oxidase[a]	1.4 ± 0.2	0.3 ± 0.1
$2\ NO + 2\ e + 2\ H^+ \rightarrow N_2O + H_2O$	NO/O_2 reductase[c]	0.7 ± 0.2	0.7 ± 0.2
$O^2 + 4\ e + 4\ H^+ \rightarrow 2\ H_2O$			
Iron storage	Ferritin	0.9 ± 0.2	1.2 ± 0.3
Redox buffering	Thioredoxin[a,d]	1.5 ± 0.2 (0.4 ± 0.1)	6.6 ± 0.6 (2.3 ± 0.2)
	Rubredoxin	1.8 ± 0.3	1.6 ± 0.4
Total[a]		10.1 ± 0.6	18.4 ± 1.4
Total corrected for genome size[e]		5.9 ± 0.4	6.4 ± 0.5

See Supplementary Table 3 for more details about gene re-annotation and enzymes comparison data.

[a]Statistically significant difference at the level of $P < 0.01$ between the two classes of methanogens.

[b]Peroxiredoxin can also reduce phospholipid hydroperoxides to repair damaged lipids.

[c]NO/O_2 reductase in methanogens was inappropriately annotated as $F_{420}H_2$ oxidase prior to this study (Supplementary Figure 3).

[d]Numbers of total and transmembrane thioredoxin proteins are indicated outside and inside the parentheses, respectively.

[e]Gene abundance after correction for genome size is shown here, and the unit is gene number per Mb of genome.

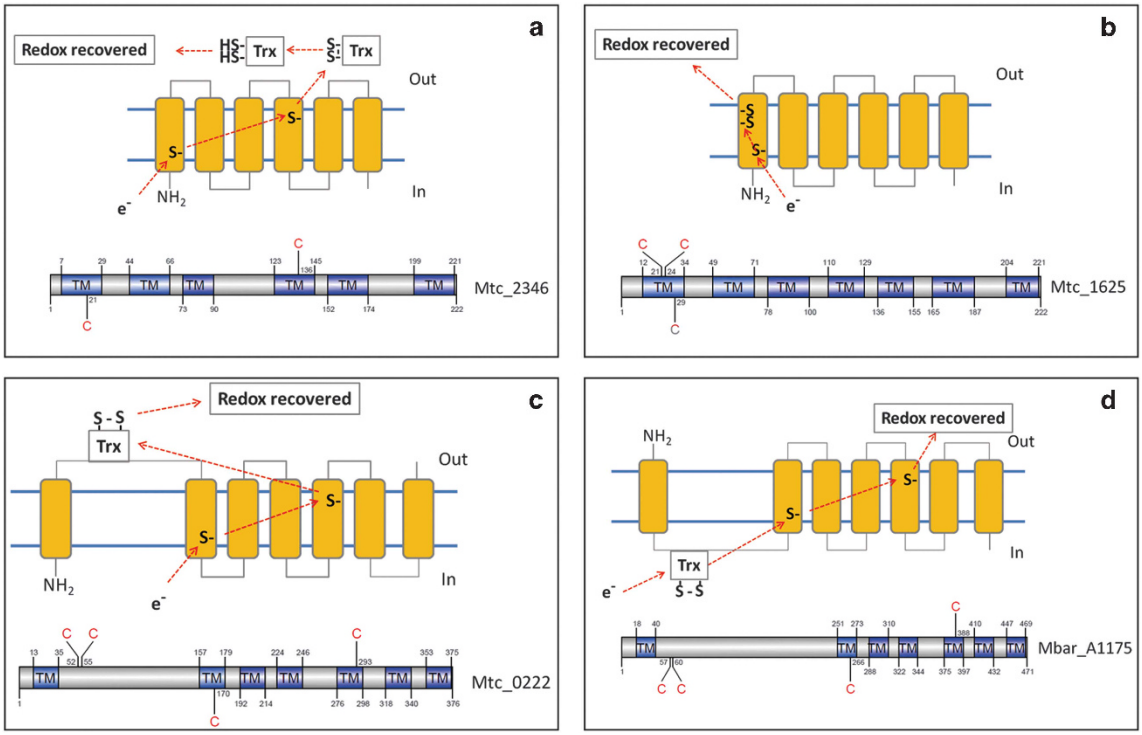

Figure 2 Predicted transmembrane structures for (**a**), Ccd-like protein using Mtc_2346 of *Methanocella conradii* as a reference; (**b**), Ccd-like protein with a transmembrane CxxC motif, using Mtc_1625 of *Methanocella conradii* as a reference; (**c**), DsbD-like protein with a periplasmic CxxC motif, using Mtc_0222 of *Methanocella conradii* as a reference; and (**d**), DsbD-like protein with a cytoplasmic CxxC motif, using Mbar_A1175 of *Methanosarcina barkeri* as a reference. Presumably, electrons could be relayed between the cytoplasmic (in) and periplasmic space (out), through those transmembrane proteins' cysteine residues located in the cellular membrane and the thioredoxin domain located either in the cytoplasmic or the periplasmic space (Krupp *et al.*, 2001; Deshmukh *et al.*, 2003). Trx, thioredoxin domain. TM, transmembrane helix. C, cysteine residues. S-, sulfide moieties of the cysteine residues. Cartoons were drawn using DOG 1.0 (Ren *et al.*, 2009). See more details in Supplementary Methods.

compared to the Class I members (Table 3 and Supplementary Table 4). A similar trend was evident for phospholipid hydroperoxides reduction mediated by the peroxiredoxins already shown in Table 3. The high enrichment of cytoplasmic S–S reduction enzymes in the Class II methanogens was consistent with the higher abundance of thioredoxins (Table 3), which were largely regenerated by thioredoxin reductases (Supplementary Table 4).

In terms of FeS assembly, most Class I methanogens could only use sulfide but not cysteine as a sulfur source, owing to the absence of genes encoding cysteine desulfurase (Liu *et al.*, 2010). In contrast, a cysteine desulfurase gene namely *iscU* was ubiquitous in the Class II methanogens, and some members even possessed an additional cysteine desulfurase gene *sufS*. This ability of using cysteine as a sulfur source for FeS assembly may ensure adaptation to oxidative environments for the Class II methanogens, as sulfide is mostly depleted under oxidative conditions (Lyu and Lu, 2015). In addition, two types of FeS carriers (that is, A-type and ApbC) were encoded by many Class II methanogens except the *Methanomicrobiales*, while only one type (that is, ApbC) was encoded by the Class I methanogens, suggesting a further adaptation of many Class II members to oxidative environments. In bacteria, there is a shift between expression of the two types of FeS carriers during the adaptation to aerobic respiration from anaerobic fermentation (Outten *et al.*, 2004). In summary, like the O_2/ROS elimination system, self-repairing genes also appear to be more enriched in the Class II methanogens than the Class I members.

Class II methanogens more frequently detected in oxidative environments

Our comparative genomic analyses suggest a potential metabolic shift from the Class I to the Class II methanogens, resulting in a richer set of antioxidant features in the latter. However, encoding more antioxidant genes does not necessarily relate to different abilities to cope with oxidative stress. To gain more insight on this matter, an environmental 16 S rRNA gene sequences survey was performed to link gene sequence identity to its corresponding habitat. If the Class II methanogens are more adapted to oxidative environments than the Class I, they should be more frequently detected in a range of oxygenated habitats.

Extracted from EnvDB, a database that links prokaryotic taxa to their habit information, a total of 212 and 485 out of ~5000 sequences could be

characterized as possessing origins from 'oxic' and 'oxic-anoxic interface' habitats, respectively (Table 4 and Supplementary Table 5) (Tamames *et al*., 2009). There was a substantial difference in the distribution of sequences affiliating with the two classes of methanogens. In particular, after normalization of sample size, sequences belonging to the Class II methanogens were nine times more frequent in oxygenated habitats than sequences of the Class I methanogens (Table 4). Importantly, this difference remained valid across a wide range of habitats including ocean, rice soil, subsurface, upland and wetland (Table 4), indicating a universal adaptation to oxic environments for the Class II methanogens. For the 'interface' sequences, the initial analysis showed no difference between the two classes of methanogens, after the sample size normalization (Table 4). However, a closer examination of the data suggested that the 'interface' sequences affiliated to the Class I methanogens were retrieved mostly in association with insects. Upon removal of all 'insect' associated sequences, sequences affiliating with the Class II methanogens were six times more frequent in the remaining 'interface' samples than sequences associated with the Class I methanogens (Table 4). Likewise, the already scarce 'oxic' sequences affiliated to the Class I methanogens were exclusively found in association with plants in rice and upland soils, suggesting that Class I methanogens found in oxygenated environments may not be exposed and adapted to oxygenic conditions but instead inhabit anoxic niches inside or near a host organism (Supplementary Table 5). In summary, the environmental data was in good agreement with the comparative genomics results, suggesting the Class II methanogens are more adapted to oxidative environments than the Class I methanogens.

Table 3 Comparison of gene abundance for enzymes repairing oxidative damage between class I and class II methanogens

Function	*Enzyme*	*Number of genes ± s.e.m.*	
		Class I	*Class II*
DNA base repair	DNA glycolyase[a]	0.7 ± 0.2	2.7 ± 0.3
	Endonuclease[a]	1.1 ± 0.1	1.6 ± 0.2
S–S recovery	Disulfide reductase (in)[a,b]	1.5 ± 0.2	6.2 ± 0.6
	Disulfide reductase (out)[a,c]	0.4 ± 0.1	2.1 ± 0.4
S = O recovery	MsrA[a,d]	0.6 ± 0.2	1.2 ± 0.2
	MsrB[a,d]	0.5 ± 0.2	0.9 ± 0.1
	Total[a]	4.7 ± 0.6	14.6 ± 1.0
FeS assembly	FeS carrier (A-type)	−	+/−[e]
	FeS carrier (ApbC)	+	+
	FeS synthesis (IscSU)	−/+[f]	+
	FeS synthesis (SufBCD)	+	+
	FeS synthesis (SufBCDES)	−	−/+[g]

See Supplementary Table 4 for more details about gene re-annotation and enzymes comparison data.
[a]Statistically significant difference at the level of $P<0.01$, except for the S = O recovery enzymes ($P<0.05$).
[b](in), cytoplasmic.
[c](out), membrane bound.
[d]Peptide methionine sulfoxide reductase MsrA/MsrB.
[e]Not present in *Methanomicrobiales*.
[f]Present in *Methanobrevibacter* and *Methanosphaera* spp. and *Methanococcus vannielii* SB.
[g]SufBCD present in all members of the Class II, but SufES were only found in *Methanohalophilus mahii* SLP and *Methanosalsum zhilinae* WeN5.

Divergence time estimated for the two methanogen classes

To gain more insight in the evolutionary history of the Class I and Class II methanogens, phylogenomic and dating analyses were conducted to infer the divergence time for the methanogens. In contrast to previous studies that considered almost all ribosomal markers, the analyses done here were based on a restricted number of ribosomal markers to minimize potential phylogenetic bias caused by horizontal gene transfer. The 22 ribosomal markers included in our analyses were considered to be inherited vertically across archaeal species (Matte-Tailliez *et al*., 2002).

In general, both the Maximum-likelihood (ML) and BI trees exhibited identical topologies at the order

Table 4 Abundance of 16 S rRNA sequences in different habitats[a]

Habitats	*Class I*	*I%*[b]	*Class II*	*II%*[b]	*I + II*	*(I + II)%*
Anoxic	935	22% (51%)	3316	78% (49%)	4215	100%
Interface	119	25% (48%)	366	75% (52%)	485	100%
Interface w/o insect	15	5% (14%)	262	95% (86%)	277	100%
Oxic	8	4% (10%)	204	96% (90%)	212	100%
Oxic-ocean	0	0 (0)	16	100% (100%)	16	100%
Oxic-rice soil	6	10% (29%)	55	90% (71%)	61	100%
Oxic-subsurface	0	0 (0)	28	100% (100%)	28	100%
Oxic-upland	2	7% (22%)	26	93% (78%)	28	100%
Oxic-wetland	0	0 (0)	79	100% (100%)	79	100%
Total	1062	21% (50%)	3886	79% (50%)	4948	100%

See Supplementary Table 5 for detailed classification of each sequence with literature referenced.
[a]All sequences were extracted from EnvDB and classified by RDP10 (See Methods). Raw habitats information for each sequence were obtained from EnvDB and then manually curated from the literature.
[b]Shown in parentheses are values normalized to sample size. For example, normalized $I_{anoxic}\% = [I_{anoxic} \times (\text{Total of II/Total of I})]/[II_{anoxic}+(I_{anoxic} \times (\text{Total of II/Total of I}))]$, and normalized II% = 100% − normalized I%.

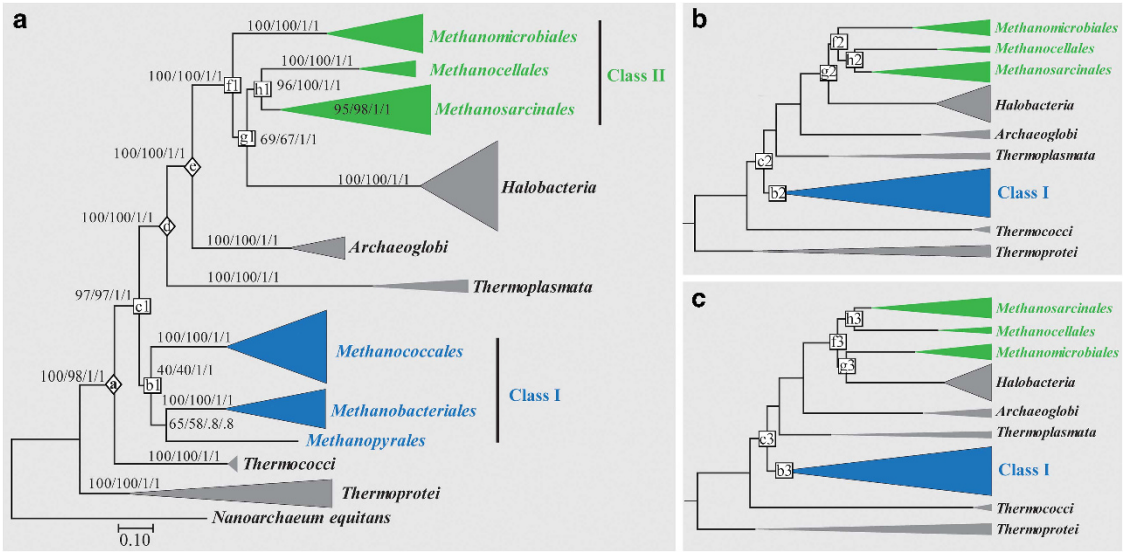

Figure 3 (**a**) Maximum-likelihood (ML) tree modeled with either 'WAG+G (4)+I' or 'LG+G (4)+I' matrix based on a concatenation of 22 ribosomal proteins sampled from methanogens *Methanopyrales*, *Methanobacteriales*, *Methanococcales*, *Methanomassiliicoccales*, *Methanomicrobiales*, *Halobacteria*, *Methanocellales* and *Methanosarcinales*, with other euryarchaeal sequences from *Archaeoglobi*, *Thermoplasmatales*, *Thermococci* and *Thermoprotei* as references (Supplementary Table 1). The tree was rooted by *Nanoarchaeum equitans*. The ribosomal proteins include Rpl2p, Rpl15p, Rpl18p, Rpl22p, Rpl23p, Rpl30p, Rpl3p, Rpl44e, Rpl4p, Rps10p, Rps13, Rps15p, Rps17e, Rps19e, Rps19p, Rps2p, Rps3p, Rps4p, Rps5p, Rps6e and Rps7p. Node values indicate bootstrap supports (first/second value for WAG/LG) for the ML tree and posterior probabilities (third/fourth value for WAG/LG) for the Bayesian tree, respectively. The bar represents the number of changes per sequence position out of a total of 3067 positions. The same tree topology on the order level was reproduced by Bayesian inference with MrBayes. Nevertheless, alternative ML tree topologies shown in (**b**) and (**c**) were also found, and the three tree topologies at the class level differed only at the phylogenetic position of *Halobacteria*. Shown in Table 5, time estimates for the indicated nodes (open square) were inferred for all the three tree topologies with internal calibration points (open diamond) derived from previous studies (Battistuzii and Hedges, 2009,Marin *et al.*, 2017).

level (Figure 3a). Consistent with previous studies, the Class I methanogens formed a monophyletic group (Bapteste *et al.*, 2005; Anderson *et al.*, 2009; Forterre, 2015; Petitjean *et al.*, 2015). This cluster was strongly supported by the BI trees, but with weak bootstrap supports by the ML trees. As already documented in previous studies (Forterre, 2015; Petitjean *et al.*, 2015), the uncertainties for the ML tree may stem from the exact placement for each of the three orders within the Class I, owing to the unstable position of *Methanopyrales*. It could either form a sister lineage with the *Methanobacteriales–Methanococcales* cluster (Bapteste *et al.*, 2005; Anderson *et al.*, 2009; Petitjean *et al.*, 2015), or with *Methanobacteriales* to the exclusion of *Methanococcales* (Forterre, 2015; Petitjean *et al.*, 2015). The Class II methanogens, however, did not form a monophyletic group. Instead, *Methanocellales* and *Methanosarcinales* formed a cluster with *Halobacteria* to the exclusion of *Methanomicrobiales* (Figure 3a). Although this topology was strongly supported by the BI trees it had only moderate support by the ML trees (Figure 3a). About 30% of the remaining ML trees either grouped the Class II methanogens into a monophyletic group (Figure 3b), to the exclusion of *Halobacteria* (Andam and Gogarten, 2011; Yutin *et al.*, 2012; Sorokin *et al.*, 2017) or recovered two monophyletic groups (Figure 3c), containing *Methanosarcinales–Methanocellales* and *Methanomicrobiales–Halobacteria*, respectively (Brochier-Armanet *et al.*, 2011; Petitjean *et al.*, 2015; Raymann *et al.*, 2015).

All three topologies were subjected to molecular dating, calibrated by three divergence time points reported previously (Battistuzii and Hedges, 2009) and re-used in a recent study (Battistuzii and Hedges, 2009; Marin *et al.*, 2017). Those divergence time points were initially derived using a Bayesian timing method with two constraints (Battistuzii and Hedges, 2009), a minimum of 3.46 Ga for the origin of methanogenesis evidenced by isotopically light carbon (Ueno *et al.*, 2006), and a maximum of 4.20 Ga divergence within Archaea inferred by the midpoint of the time range estimated for the last ocean-vaporizing event (Sleep *et al.*, 1989). It was found that ancestors of the Class I methanogens first branched off the euryarchaeal tree at 3.4–3.3 Ga (nodes c1–c3) and then started to diverge into the three orders at 3.2–3.1 Ga (nodes b1–b3) (Table 5). Despite the uncertain topologies regarding the Class II methanogens, their divergence time estimates remained relatively stable, that is, they branched off the euryarchaeal tree at 2.3–2.2 Ga (nodes f1–f3). Likewise, their further divergence into *Methanocellales* and *Methanosarcinales* remained almost unchanged at ~2.0 Ga (nodes h1–h3). Depending on its phylogenetic placements, *Halobacteria* diverged from the Class II methanogens from 2.4–

Table 5 Divergence times (Ma) and confidence intervals (CI) among the euryarchaea

Node[a]	*Time estimates (CI)*		
	Ref	*ML-WAG/BI-WAG*	*ML–LG/BI–LG*[b]
a	3594 (3691–3503)	-	-
b1	3313 (3388–3232)	3178 (3023–3333)/3176 (3022–3330)	3185 (3033–3336)
b2	-	3153 (2975–3330)	3169 (2980–3354)
b3	-	3153 (2954–351)	3183 (3035–3333)
c1	3468 (3490–3460)	3375 (3166–3583)/3374 (3168–3580)	3366 (3153–3578)
c2	-	3344 (3160–3594)	3340 (3160–3594)
c3	-	3343 (3160–3594)	3361 (3160–3594)
d	3160 (3257–3056)	-	-
e	2799 (2936–2656)	-	-
f1	-	2347 (2134–2560)/2351 (2141–2563)	2334 (2120–2547)
f2	-	2245 (2050–2439)	2245 (2030–2460)
f3	-	2293 (2093–2494)	2287 (2086–2487)
g1	-	2185 (1934–2436)/2186 (1938–2425)	2180 (1929–2431)
g2	-	2387 (2222–2552)	2384 (2202–2567)
g3	-	2162 (1903–2421)	2153 (1893–2413)
h1	-	2007 (1712–2302)/2007 (1716–2298)	1994 (1699–2289)
h2	-	2003 (1750–2257)	2004 (1725–2283)
h3	-	2043 (1771–2314)	2045 (1775–2315)

Both the Maximum-likelihood (ML) and Bayesian inference (BI) trees from Figure 3 were first subjected to the RelTime analysis by Mega 7 using either the WAG or LG model as described in the methods. This resulted in relative node ages, which were then transformed into absolute ages using calibration points for nodes a, d and e reported previously (Battistuzii and Hedges, 2009; Marin *et al.*, 2017). Time estimates in the Ref column corresponding to nodes b1 and c1 were not used as calibration points, but are listed here to show that their ages were comparable to the corresponding node ages estimated in this study. This suggests use of calibration points here did not severely distort the divergence times for the otherwise conserved nodes consistently supported by phylogenomic studies.

[a]The numbers 1, 2 and 3 after the node letters corresponds to the three ML topologies shown in Figures 3a–c, respectively, concerning the different phylogenetic positions of *Halobacteria*.

[b]When rounding up, time estimates are identical for the ML–LG and BI–LG.

2.1 Ga (nodes g1–g3). Although using a restricted ribosomal proteins' data set did not resolve the uncertainties regarding the exact phylogenetic positions of the Class II methanogens, the results were able to provide time estimates indicating that the divergence of the Class I and Class II methanogens might have occurred before and around the time of the Great Oxygenation Event, respectively.

Conclusions

In this study, comparative genomic analyses and environmental sequences surveys identified two distinct methanogen clusters, corresponding to the Class I and Class II methanogens, respectively, as proposed previously based on phylogenomic studies (Brochier-Armanet *et al.*, 2011; Petitjean *et al.*, 2015). The results in the present study suggested that the Class I methanogens had limited abilities for oxidative adaptation. In contrast, the Class II methanogens possessed expanded genomic features potentially enabling better adaptation to oxidative environments. Three general evolutionary mechanisms towards a stronger tolerance to oxidative stress for methanogens at the class level could be envisaged from our analyses. The first is the usage of enzymes producing less ROS or enhancing ROS removal in largely unchanged pathways, which has been observed in the evolution of electron bifurcation-based hydrogenotrophic methanogenesis and O_2/ROS elimination pathways. The second is to employ a completely new pathway resulting in less ROS production, which has been found in the shift from an electron bifurcation to a cytochrome/methanophenazine based methanogenesis pathway. The third is the expansion and diversification upon a core antioxidant system, which has been seen in the O_2/ROS elimination and self-repairing pathways.

Our phylogenomic and dating analyses further suggested that the Class I methanogens might have evolved before the Great Oxygenation Event. The Class II methanogens, on the other hand, might have evolved later, possibly expanding their antioxidant features as a response to the abruptly elevated oxidative stress. This would not only protect them from an increasingly oxidized Earth but enabled access to nickel available in the oxidized layer during the 'nickel famine' that began at ~2.5 Ga (Konhauser *et al.*, 2009). Alternatively, it is possible that the metabolic changes between the two methanogen classes observed here were due to recent niche specialization rather than an ancient adaptation to oxygenation. However, this would seem counterintuitive given that the lately evolved Class II methanogens mainly modified or expanded upon the many antioxidant features already present in the early evolved Class I methanogens, which comprise many hyperthermophilic organisms that thrive in habitats resembling those environments where microbial ancestors first arose (Boussau *et al.*, 2008; Liu and Whitman, 2008). Nevertheless, studies on

ancient gene reconstruction may shed more light on the evolutionary history of both methanogens and their antioxidant systems. On the other hand, discoveries of new methanogen lineages will greatly contribute to this effort, especially those that possess ancient metabolisms. Indeed, new methanogens are continued to be found, including but perhaps not limited to the seventh methanogen order *Methanomassiliicoccales* (Dridi *et al.*, 2012; Borrel *et al.*, 2013), the *Candidatus* 'Methanofastidiosum' belonging to the WSA2 euryarchaeal class (Riviere *et al.*, 2009; Nobu *et al.*, 2016), the *Candidatus* 'Methanonatronarchaeia' representing the halophilic SA1 euryarchaeal group (Eder *et al.*, 2002; Sorokin *et al.*, 2017), and even some putative methanogens outside the *Euryarchaeota* (Evans *et al.*, 2015; Vanwonterghem *et al.*, 2016). Considering that most of those newly discovered methanogens appear to be methylotrophic, it may be speculated that they evolved later since the main substrates available in ancient environments would have favored methanogenic growth on H_2 and CO_2 (Martin, 2011).

Conflict of Interest

The authors declare no conflict of interest.

Acknowledgements

We appreciate William B Whitman for critical comments and proofreading. We thank Rudolf K Thauer, Ralf Conrad and the anonymous reviewers for critical comments and suggestions to this work. During the manuscript revision, much calculation and analysis work was accomplished in the laboratory of William B Whitman. We appreciate his generous support and assistance. This work was supported by the National Natural Science Foundation of China (41630857).

Author contributions

ZL and YL conceived the study; ZL designed the study and analyzed the data; ZL and YL wrote the paper. Both authors read and approved the final manuscript.

References

Andam CP, Gogarten JP. (2011). Biased gene transfer in microbial evolution. *Nat Rev Microbiol* **9**: 543–555.

Anderson I, Ulrich LE, Lupa B, Susanti D, Porat I, Hooper SD *et al.* (2009). Genomic characterization of *Methanomicrobiales* reveals three classes of methanogens. *PLoS One* **4**: e5797.

Angel R, Matthies D, Conrad R. (2011). Activation of methanogenesis in arid biological soil crusts despite the presence of oxygen. *PLoS One* **6**: e20453.

Angel R, Claus P, Conrad R. (2012). Methanogenic archaea are globally ubiquitous in aerated soils and become active under wet anoxic conditions. *ISME J* **6**: 847–862.

Åslund F, Berndt KD, Holmgren A. (1997). Redox potentials of glutaredoxins and other thiol-disulfide oxidoreductases of the thioredoxin superfamily determined by direct protein-protein redox equilibria. *J Biol Chem* **272**: 30780–30786.

Balmer Y, Vensel WH, Tanaka CK, Hurkman WJ, Gelhaye E, Rouhier N *et al.* (2004). Thioredoxin links redox to the regulation of fundamental processes of plant mitochondria. *Proc Natl Acad Sci USA* **101**: 2642–2647.

Bapteste E, Brochier C, Boucher Y. (2005). Higher-level classification of the Archaea: evolution of methanogenesis and methanogens. *Archaea* **1**: 353–363.

Battistuzii FU, Hedges SB. (2009). Archaebacteria. In: Hedges SB, Kumar S (eds). *The Timetree of Life*. Oxford University Press: New York, NY, USA, pp 101–105.

Battistuzzi FU, Feijao A, Hedges SB. (2004). A genomic timescale of prokaryote evolution: insights into the origin of methanogenesis, phototrophy, and the colonization of land. *BMC Evol Biol* **4**: 44.

Borrel G, O'Toole PW, Harris HM, Peyret P, Brugere JF, Gribaldo S. (2013). Phylogenomic data support a seventh order of methylotrophic methanogens and provide insights into the evolution of methanogenesis. *Genome Biol Evol* **5**: 1769–1780.

Bousquet P, Ciais P, Miller JB, Dlugokencky EJ, Hauglustaine DA, Prigent C *et al.* (2006). Contribution of anthropogenic and natural sources to atmospheric methane variability. *Nature* **443**: 439–443.

Boussau B, Blanquart S, Necsulea A, Lartillot N, Gouy M. (2008). Parallel adaptations to high temperatures in the Archaean eon. *Nature* **456**: 942–945.

Brochier-Armanet C, Forterre P, Gribaldo S. (2011). Phylogeny and evolution of the Archaea: one hundred genomes later. *Curr Opin Microbiol* **14**: 274–281.

Buckel W, Thauer RK. (2012). Energy conservation via electron bifurcating ferredoxin reduction and proton/Na+ translocating ferredoxin oxidation. *BBA-Bioenergetics* **1827**: 94–113.

Catlett JL, Ortiz AM, Buan NR. (2015). Rerouting Cellular electron flux to increase the rate of biological methane production. *Appl Environ Microbiol* **81**: 6528–6537.

Catling DC, Zahnle KJ, McKay CP. (2001). Biogenic methane, hydrogen escape, and the irreversible oxidation of early earth. *Science* **293**: 839–843.

Cole JR, Wang Q, Cardenas E, Fish J, Chai B, Farris RJ *et al.* (2009). The Ribosomal Database Project: improved alignments and new tools for rRNA analysis. *Nucleic Acids Res* **37**: D141–D145.

Dalhus B, Laerdahl JK, Backe PH, Bjoras M. (2009). DNA base repair–recognition and initiation of catalysis. *FEBS Microbiol Rev* **33**: 1044–1078.

Deshmukh M, Turkarslan S, Astor D, Valkova-Valchanova M, Daldal F. (2003). The Dithiol:disulfide oxidoreductases DsbA and DsbB of *Rhodobacter capsulatus* are not directly involved in cytochrome c biogenesis, but their inactivation restores the cytochrome c biogenesis defect of CcdA-Null Mutants. *J Bacteriol* **185**: 3361–3372.

Djaman O, Outten FW, Imlay JA. (2004). Repair of oxidized iron-sulfur clusters in *Escherichia coli*. *J Biol Chem* **279**: 44590–44599.

Dridi B, Fardeau M-L, Ollivier B, Raoult D, Drancourt M. (2012). *Methanomassiliicoccus luminyensis* gen. nov., sp. nov., a methanogenic archaeon isolated from human faeces. *Int J Syst Evol Microbiol* **62**: 1902–1907.

Eder W, Schmidt M, Koch M, Garbe-Schonberg D, Huber R. (2002). Prokaryotic phylogenetic diversity and corresponding geochemical data of the brine-seawater interface of the Shaban Deep, Red Sea. *Environ Microbiol* **4**: 758–763.

Erkel C, Kube M, Reinhardt R, Liesack W. (2006). Genome of Rice Cluster I *Archaea* - the key methane producers in the rice rhizosphere. *Science* **313**: 370–372.

Evans PN, Parks DH, Chadwick GL, Robbins SJ, Orphan VJ, Golding SD *et al.* (2015). Methane metabolism in the archaeal phylum Bathyarchaeota revealed by genome-centric metagenomics. *Science* **350**: 434–438.

Fetzer S, Bak F, Conrad R. (1993). Sensitivity of methanogenic bacteria from paddy soil to oxygen and desiccation. *FEMS Microbiol Ecol* **12**: 107–115.

Fetzer S, Conrad R. (1993). Effect of redox potential on Methanogenesis by *Methanosarcina barkeri*. *Arch Microbiol* **160**: 108–113.

Forterre P. (2015). The universal tree of life: an update. *Front Microbiol* **6**: 717.

Gomes CM, Giuffrè A, Forte E, Vicente JB, Saraiva LgM, Brunori M *et al.* (2002). A novel type of nitric-oxide reductase. *J Biol Chem* **277**: 25273–25276.

Gort AS, Imlay JA. (1998). Balance between endogenous superoxide stress and antioxidant defenses. *J Bacteriol* **180**: 1402–1410.

Hausrath EM, Liermann LJ, House CH, Ferry JG, Brantley SL. (2007). The effect of methanogen growth on mineral substrates: will Ni markers of methanogen-based communities be detectable in the rock record? *Geobiology* **5**: 49–61.

Hillmann F, Fischer RJ, Saint-Prix F, Girbal L, Bahl H. (2008). PerR acts as a switch for oxygen tolerance in the strict anaerobe *Clostridium acetobutylicum*. *Mol Microbiol* **68**: 848–860.

Imlay JA. (2002). How oxygen damages microbes: oxygen tolerance and obligate anaerobiosis. *Advances in Microbial Physiology*. Academic Press: London, UK, pp 111–153.

Imlay JA. (2008). Cellular defenses against superoxide and hydrogen peroxide. *Annu Rev Biochem* **77**: 755–776.

Imlay JA. (2013). The molecular mechanisms and physiological consequences of oxidative stress: lessons from a model bacterium. *Nat Rev Microbiol* **11**: 443–454.

Kaster AK, Moll J, Parey K, Thauer RK. (2011). Coupling of ferredoxin and heterodisulfide reduction via electron bifurcation in hydrogenotrophic methanogenic archaea. *Proc Natl Acad Sci USA* **108**: 2981–2986.

Kasting JF. (1993). Earth's early atmosphere. *Science* **259**: 920–926.

Kasting JF. (2004). When methane made climate. *Sci Am* **291**: 78–85.

Katoh K, Standley DM. (2013). MAFFT multiple sequence alignment software version 7: improvements in performance and usability. *Mol Biol Evol* **30**: 772–780.

Kearse M, Moir R, Wilson A, Stones-Havas S, Cheung M, Sturrock S *et al.* (2012). Geneious Basic: an integrated and extendable desktop software platform for the organization and analysis of sequence data. *Bioinformatics* **28**: 1647–1649.

Kiener A, Leisinger T. (1983). Oxygen sensitivity of methanogenic bacteria. *Syst Appl Microbiol* **4**: 305–312.

Klüber HD, Conrad R. (1998). Effects of nitrate, nitrite, NO and N_2O on methanogenesis and other redox processes in anoxic rice field soil. *FEMS Microbiol Ecol* **25**: 301–318.

Konhauser KO, Pecoits E, Lalonde SV, Papineau D, Nisbet EG, Barley ME *et al.* (2009). Oceanic nickel depletion and a methanogen famine before the Great Oxidation Event. *Nature* **458**: 750–753.

Krupp R, Chan C, Missiakas D. (2001). DsbD-catalyzed transport of electrons across the membrane of *Escherichia coli*. *J Biol Chem* **276**: 3696–3701.

Kulkarni G, Kridelbaugh DM, Guss AM, Metcalf WW. (2009). Hydrogen is a preferred intermediate in the energy-conserving electron transport chain of *Methanosarcina barkeri*. *Proc Natl Acad Sci USA* **106**: 15915–15920.

Kumar S, Hedges SB. (2016). Advances in time estimation methods for molecular data. *Mol Biol Evol* **33**: 863–869.

Kumar S, Stecher G, Tamura K. (2016). MEGA7: molecular evolutionary genetics analysis version 7.0 for bigger datasets. *Mol Biol Evol* **33**: 1870–1874.

Lin I-J, Gebel EB, Machonkin TE, Westler WM, Markley JL. (2005). Changes in hydrogen-bond strengths explain reduction potentials in 10 rubredoxin variants. *Proc Natl Acad Sci USA* **102**: 14581–14586.

Liu Y, Whitman WB. (2008). Metabolic, phylogenetic, and ecological diversity of the methanogenic archaea. *Ann N Y Acad Sci* **1125**: 171–189.

Liu Y, Sieprawska-Lupa M, Whitman WB, White RH. (2010). Cysteine is not the sulfur source for iron-sulfur cluster and methionine biosynthesis in the methanogenic archaeon *Methanococcus maripaludis*. *J Biol Chem* **285**: 31923–31929.

Lollar BS, Onstott TC, Lacrampe-Couloume G, Ballentine CJ. (2014). The contribution of the Precambrian continental lithosphere to global H_2 production. *Nature* **516**: 379–382.

Lu J, Holmgren A. (2014). The thioredoxin antioxidant system. *Free Radic Biol Med* **66**: 75–87.

Lyu Z, Lu Y. (2015). Comparative genomics of three *Methanocellales* strains reveal novel taxonomic and metabolic features. *Environ Microbiol Rep* **7**: 526–537.

Ma K, Lu Y. (2011). Regulation of microbial methane production and oxidation by intermittent drainage in rice field soil. *FEMS Microbiol Ecol* **75**: 446–456.

Major TA, Burd H, Whitman WB. (2004). Abundance of 4Fe-4S motifs in the genomes of methanogens and other prokaryotes. *FEMS Microbiol Lett* **239**: 117–123.

Manevich Y, Sweitzer T, Pak JH, Feinstein SI, Muzykantov V, Fisher AB. (2002). 1-Cys peroxiredoxin overexpression protects cells against phospholipid peroxidation-mediated membrane damage. *Proc Natl Acad Sci USA* **99**: 11599–11604.

Marin J, Battistuzzi FU, Brown AC, Hedges SB. (2017). The Timetree of Prokaryotes: New Insights into Their Evolution and Speciation. *Mol Biol Evol* **34**: 437–446.

Martin WF. (2011). Hydrogen, metals, bifurcating electrons, and proton gradients: The early evolution of biological energy conservation. *FEBS Lett* **586**: 485–493.

Massey V. (1994). Activation of molecular oxygen by flavins and flavoproteins. *J Biol Chem* **269**: 22459–22462.

Matte-Tailliez O, Brochier C, Forterre P, Philippe H. (2002). Archaeal phylogeny based on ribosomal proteins. *Mol Biol Evol* **19**: 631–639.

McCarver AC, Lessner DJ. (2014). Molecular characterization of the thioredoxin system from *Methanosarcina acetivorans*. *FEBS J* **281**: 4598–4611.

Miller MA, Pfeiffer W, Schwartz T. (2010). Creating the CIPRES Science Gateway for inference of large phylogenetic trees. *Gateway Computing Environments Workshop (GCE)*; 14-14 Nov. 2010.

Müller F. (1987). Flavin radicals: chemistry and biochemistry. *Free Radic Biol Med* **3**: 215–230.

Neilands JB. (1993). Siderophores. *Arch Biochem Biophys* **302**: 1–3.

Nisbet EG, Sleep NH. (2001). The habitat and nature of early life. *Nature* **409**: 1083–1091.

Nobu MK, Narihiro T, Kuroda K, Mei R, Liu W-T. (2016). Chasing the elusive Euryarchaeota class WSA2: genomes reveal a uniquely fastidious methyl-reducing methanogen. *ISME J* **10**: 2478–2487.

Outten FW, Djaman O, Storz G. (2004). A suf operon requirement for Fe-S cluster assembly during iron starvation in *Escherichia coli*. *Mol Microbiol* **52**: 861–872.

Pavlov AA, Kasting JF, Brown LL, Rages KA, Freedman R. (2000). Greenhouse warming by CH4 in the atmosphere of early Earth. *J Geophys Res* **105**: 11981–11990.

Petitjean C, Deschamps P, López-García P, Moreira D, Brochier-Armanet C. (2015). Extending the conserved phylogenetic core of archaea disentangles the evolution of the third domain of life. *Mol Biol Evol* **32**: 1242–1254.

Raymann K, Brochier-Armanet C, Gribaldo S. (2015). The two-domain tree of life is linked to a new root for the Archaea. *Proc Natl Acad Sci USA* **112**: 6670–6675.

Ren J, Wen L, Gao X, Jin C, Xue Y, Yao X. (2009). DOG 1.0: illustrator of protein domain structures. *Cell Res* **19**: 271–273.

Riviere D, Desvignes V, Pelletier E, Chaussonnerie S, Guermazi S, Weissenbach J *et al.* (2009). Towards the definition of a core of microorganisms involved in anaerobic digestion of sludge. *ISME J* **3**: 700–714.

Rodrigues R, Vicente JB, Félix R, Oliveira S, Teixeira M, Rodrigues-Pousada C. (2006). Desulfovibrio gigas flavodiiron protein affords protection against nitrosative stress in vivo. *J Bacteriol* **188**: 2745–2751.

Ronquist F, Huelsenbeck JP. (2003). MrBayes 3: Bayesian phylogenetic inference under mixed models. *Bioinformatics* **19**: 1572–1574.

Schlegel K, Welte C, Deppenmeier U, Müller V. (2012). Electron transport during aceticlastic methanogenesis by *Methanosarcina acetivorans* involves a sodium-translocating Rnf complex. *FEBS J* **279**: 4444–4452.

Seedorf H, Dreisbach A, Hedderich R, Shima S, Thauer RK. (2004). $F_{420}H_2$ oxidase (FprA) from *Methanobrevibacter arboriphilus*, a coenzyme F420-dependent enzyme involved in O_2 detoxification. *Arch Microbiol* **182**: 126–137.

Seedorf H, Hagemeier CH, Shima S, Thauer RK, Warkentin E, Ermler U. (2007). Structure of coenzyme $F_{420}H_2$ oxidase (FprA), a di-iron flavoprotein from methanogenic Archaea catalyzing the reduction of O_2 to H_2O. *FEBS J* **274**: 1588–1599.

Silaghi-Dumitrescu R, Ng KY, Viswanathan R, Kurtz DM. (2005). A flavo-diiron protein from *Desulfovibrio vulgaris* with oxidase and nitric oxide reductase activities. Evidence for an in vivo nitric oxide scavenging function†. *Biochemistry* **44**: 3572–3579.

Sleep NH, Zahnle KJ, Kasting JF, Morowitz HJ. (1989). Annihilation of ecosystems by large asteroid impacts on the early Earth. *Nature* **342**: 139–142.

Sorokin DY, Makarova KS, Abbas B, Ferrer M, Golyshin PN, Galinski EA *et al.* (2017). Discovery of extremely halophilic, methyl-reducing euryarchaea provides insights into the evolutionary origin of methanogenesis. *Nat Microbiol* **2**: 17081.

Spring S, Scheuner C, Lapidus A, Lucas S, Glavina Del Rio T, Tice H *et al.* (2010). The genome sequence of *Methanohalophilus mahii* SLP(T) reveals differences in the energy metabolism among members of the *Methanosarcinaceae* inhabiting freshwater and saline environments. *Archaea* **2010**: 690737.

Stamatakis A, Hoover P, Rougemont J. (2008). A rapid bootstrap algorithm for the RAxML web servers. *Syst Biol* **57**: 758–771.

Susanti D, Wong JH, Vensel WH, Loganathan U, DeSantis R, Schmitz RA *et al.* (2014). Thioredoxin targets fundamental processes in a methane-producing archaeon, *Methanocaldococcus jannaschii*. *Proc Natl Acad Sci USA* **111**: 2608–2613.

Susanti D, Loganathan U, Mukhopadhyay B. (2016). A novel F420-dependent thioredoxin reductase gated by low potential FAD: a tool for redox regulation in an anaerobe. *J Biol Chem* **291**: 23084–23100.

Tamames J, Pignatelli M, Moya A. (2009). EnvDB, a database for describing the environmental distribution of prokaryotic taxa. *Environ Microbiol Rep* **1**: 191–197.

Tamura K, Battistuzzi FU, Billing-Ross P, Murillo O, Filipski A, Kumar S. (2012). Estimating divergence times in large molecular phylogenies. *Proc Natl Acad Sci USA* **109**: 19333–19338.

Thauer RK, Kaster AK, Seedorf H, Buckel W, Hedderich R. (2008). Methanogenic archaea: ecologically relevant differences in energy conservation. *Nat Rev Microbiol* **6**: 579–591.

Thauer RK, Kaster A-K, Goenrich M, Schick M, Hiromoto T, Shima S. (2010). Hydrogenases from methanogenic archaea, nickel, a novel cofactor, and H_2 storage. *Annu Rev Biochem* **79**: 507–536.

Touati D, Jacques M, Tardat B, Bouchard L, Despied S. (1995). Lethal oxidative damage and mutagenesis are generated by iron in delta fur mutants of *Escherichia coli*: protective role of superoxide dismutase. *J Bacteriol* **177**: 2305–2314.

Ueki A, Ono K, Tsuchiya A, Ueki K. (1997). Survival of methanogens in airdried paddy field soil and their heat tolerance. *Water Sci Technol* **36**: 517–522.

Ueno Y, Yamada K, Yoshida N, Maruyama S, Isozaki Y. (2006). Evidence from fluid inclusions for microbial methanogenesis in the early Archaean era. *Nature* **440**: 516–519.

Vanwonterghem I, Evans PN, Parks DH, Jensen PD, Woodcroft BJ, Hugenholtz P *et al.* (2016). Methylotrophic methanogenesis discovered in the archaeal phylum Verstraetearchaeota. *Nat Microbiol* **1**: 16170.

Walling C. (1975). Fenton's reagent revisited. *Acc Chem Res* **8**: 125–131.

Weissbach H, Resnick L, Brot N. (2005). Methionine sulfoxide reductases: history and cellular role in protecting against oxidative damage. *Biochim Biophys Acta* **1703**: 203–212.

Welander PV, Metcalf WW. (2005). Loss of the mtr operon in *Methanosarcina* blocks growth on methanol, but not methanogenesis, and reveals an unknown methanogenic pathway. *Proc Natl Acad Sci USA* **102**: 10664–10669.

Wordsworth R, Pierrehumbert R. (2013). Hydrogen-nitrogen greenhouse warming in Earth's early atmosphere. *Science* **339**: 64–67.

Yan Z, Wang M, Ferry JG. (2017). A ferredoxin- and $F_{420}H_2$-dependent, electron-bifurcating, heterodisulfide reductase with homologs in the domains bacteria and Archaea. *mBio* **8**: e02285–16.

Yuan Y, Conrad R, Lu Y. (2011). Transcriptional response of methanogen mcrA genes to oxygen exposure of rice field soil. *Environ Microbiol Rep* **3**: 320–328.

Yutin N, Puigbò P, Koonin EV, Wolf YI. (2012). Phylogenomics of prokaryotic ribosomal proteins. *PLoS One* **7**: e36972.

Supplementary Information accompanies this paper on The ISME Journal website (http://www.nature.com/ismej)